Exchange bias and training effect in $NiCr_2O_4/Cr_2O_3$ composite

Wang Liguang, Zhu Changming, Tian Zhaoming, and Yuan Songliu[a)]
School of Physics, Huazhong University of Science and Technology, Wuhan 430074, People's Republic of China

(Received 12 May 2015; accepted 19 August 2015)

$NiCr_2O_4/Cr_2O_3$ system with ferrimagnetic spinel and antiferromagnetic transition metal oxide has been firstly synthesized by a chemical co-precipitation method. Magnetic measurements on this system also exhibit the exchange bias (EB) and training effect for the first time. EB effect with evident shift of coercive field and remnant magnetization can be detected at low temperature after field cooling from 350 K. The EB field can reach about 2037 Oe and the magnetization shift is as large as 0.129 emu/g at 10 K. Furthermore, EB effect recedes gradually with temperature increasing and disappears at about 70 K. In this process, EB field decreases with a linear dependence on the magnetization shift. This EB behavior is discussed according to the disordered regions existed at the interface between $NiCr_2O_4$ and Cr_2O_3. In addition, we have analyzed the training effect, which indicates the coexistence of two distinct forms of training mechanism during cycle procedure. One is concerned with an athermal impact resulting in the abrupt single cycle training and the other is gradual reduction of EB field during the subsequent cycles due to the conventional thermal activation mechanism.

I. INTRODUCTION

Exchange bias (EB) effect is usually exhibited in ferromagnetic/antiferromagnetic systems.[1,2] It is one of the important phenomena associated with exchange anisotropy. The typical characteristic is horizontal shift of hysteresis loops after the material is cooled with an external field from a higher temperature. EB effect was firstly discovered in passivated Co–CoO nanoparticles by Meiklejohn and Bean about 50 years ago.[3] Afterward, it has been intensively investigated in theoretical and experimental aspects due to the extensive applications in the field of advanced technology, for example, data storage as spintronic devices, magnetic recording media and so on.[4,5] EB effect can be essentially influenced by the initial temperature and the applied magnetic field during the field cooling process. Thus, training effect is another meaningful characteristic accompanied with EB effect and it reveals a strong dependence on thermal and magnetic histories of EB effect.[6] The consecutive hysteresis loop measurement after field cooling presents a decrease in EB field (H_{EB}) with ordinal measurement cycles.[7] In general, the understanding of training effect can help to study EB effect, and on other side, the study of training effect may require the exact of EB effect.

During the past decades, reports on EB effect were mainly focused on multilayer film system.[8] Some particle systems have been studied recently because of the ferromagnetic–antiferromagnetic exchange interactions, which can be useful to break the superparamagnetic limit in nanoparticles.[9,10] In addition, a series of composites containing transition metal particles and their native oxides, for example Ni–NiO,[11] have also been emphasized. Nevertheless, the system of transition metal oxides and the corresponding ferrimagnetic spinel is less investigated. $NiCr_2O_4$ is a spinel ferrimagnetic material with applications in various devices. Detailed magnetic studies of polycrystalline $NiCr_2O_4$ have been reported just in a few papers.[12,13] The corresponding transition metal oxide Cr_2O_3 has an antiferromagnetic order at 307 K and there is also rarely reports to study the magnetic effect.[14] From the above discussion, we speculate that the composite with ferrimagnetic $NiCr_2O_4$ and antiferromagnetic Cr_2O_3 may exhibit some meaningful magnetic effect.

In our research, we have firstly synthesized the $NiCr_2O_4/Cr_2O_3$ system through co-precipitation method. On this basis, we study the EB effect and training effect with different measurement conditions. EB effect is detected at low temperature and it decreases with increasing temperature. It also increases to saturation when enough high cooling field is applied. During the increasing of temperature and cooling field, EB field (H_{EB}) has a similar tendency with the shift of remnant magnetization (M_{shift}). In addition, training effect is explained by two forms of training mechanism during cycle procedure.

II. EXPERIMENTAL PROCEDURE

In this synthesis, $NiCr_2O_4/Cr_2O_3$ (1:4) composite was prepared by the chemical co-precipitation method. As described in previous literature,[15] high-pure nickel nitrate

Contributing Editor: Michael E. McHenry
[a)]Address all correspondence to this author.
e-mail: yuansl@hust.edu.cn
DOI: 10.1557/jmr.2015.272

 © Materials Research Society 2015

https://doi.org/10.1557/jmr.2015.272 Published online by Cambridge University Press

$[Ni(NO_3)_2{\cdot}6H_2O]$, chromic nitrate $[Cr(NO_3)_3{\cdot}9H_2O]$ and ammonium bicarbonate $[NH_4HCO_3]$ were used as the staring raw materials. Stoichiometric amounts of nickel nitrate and chromic nitrate were dissolved in distilled water at first. Subsequently, ammonium bicarbonate solution with appropriate content was slowly added to the upper mixture solution under constant stirring. During this process, the solution was gradually changed to suspension. After that, the obtained suspension was washed repeatedly using diluted water. Then, the suspension was dried in air at 120 °C to form precursor powders. Finally, after ground adequately for 1 h, the powders were sintered in air for 3 h with 900 °C, obtaining the $NiCr_2O_4/Cr_2O_3$ composite.

X-ray diffraction (XRD) pattern of the composite was collected on a Philips Panalytical X'Pert diffractometer (PANalytical, Almelo, Netherlands) equipped with a Cu K_α radiation source. The morphology and stoichiometry were verified by scanning electron microscope (SEM) and energy dispersive spectrometer (EDS) through a JSM-5610LV (JEOL, Tokyo, Japan). Magnetic measurements were carried out using a commercial Physical Property Measurement System (Quantum Design, San Diego, California).

III. RESULTS AND DISCUSSION

Figure 1(a) shows the XRD pattern of $NiCr_2O_4/Cr_2O_3$ composite. Two sets of diffraction pattern corresponding to $NiCr_2O_4$ (cycle) and Cr_2O_3 (diamond) can be indexed without other impurity. EDS data in Fig. 1(c) and the right inset table confirm the stoichiometry with 1:4. Considering the phase formation temperature of $NiCr_2O_4$ is higher than that of Cr_2O_3, we speculate that Ni cations react with part of Cr cations to form $NiCr_2O_4$ phase leaving the other Cr cations develop to Cr_2O_3 phase. In other words, with the special chemical synthesis method and thermal treatment, Ni cations doped in Cr cations separate the phases into ferrimagnetic $NiCr_2O_4$ and antiferromagnetic Cr_2O_3 phases by a local arrangement of the Ni and Cr cations. To confirm this, the XRD pattern of pure $NiCr_2O_4$ synthesized by the same method is shown in Fig. 1(b). In addition, the micrograph shown in the left inset of Fig. 1(c) displays the morphology of $NiCr_2O_4/Cr_2O_3$ composite. As analyzed and calculated, $NiCr_2O_4$ particles with grain size of about 50 nm are embedded in Cr_2O_3 of about 250 nm. It can further confirm that the $NiCr_2O_4$ phase is separated out from the Cr_2O_3 phase. They also prove that the ferrimagnetic $NiCr_2O_4$ and antiferromagnetic Cr_2O_3 can be coexistent in the system synthesized by the co-precipitation method.

The temperature dependent magnetization under different magnetic field with zero-field-cooled (ZFC) and field-cooled (FC) processes are plotted in Fig. 2. From Fig. 2(a), we can find that magnetization curves have a steep increase near 75 K accompanied with a clear peak

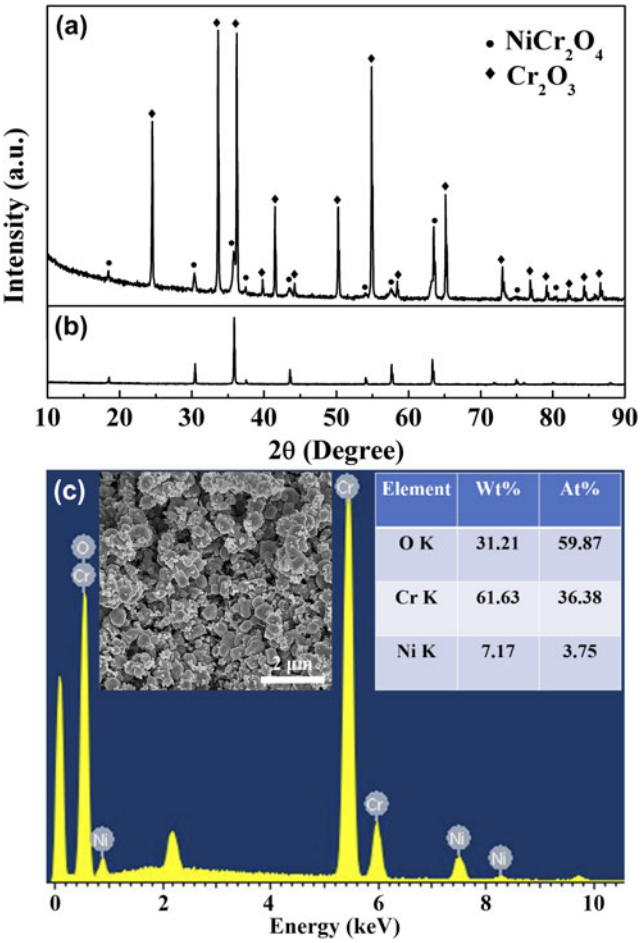


FIG. 1. (a) XRD pattern of the $NiCr_2O_4/Cr_2O_3$ system. (b) XRD pattern of the pure $NiCr_2O_4$ phase. (c) EDS spectrum of $NiCr_2O_4/Cr_2O_3$ system. The left inset is the SEM micrograph and the right inset is the proportion values of elements.

in ZFC around 68 K associated with the ferrimagnetic transition and a subtle anomaly in FC at 30 K marked with the spiral magnetic order. It is very qualitatively similar to the previous data about $NiCr_2O_4$.[12,13] The magnetization curves with high applied field of 40 kOe showed in Fig. 2(b) exhibit a broad cusp near 305 K corresponding to the antiferromagnetic orders of Cr_2O_3. In addition, as temperature decreases below the temperature about 65 K, the ZFC curve does not follow the same path as the FC curve. The irreversibility between ZFC and FC curves reveals that there are some frozen moments in the sample. Since $NiCr_2O_4$ can be separated from Cr_2O_3, an intermediate structural disorder layer including anisotropy can be formed because of the chemical roughness and the intermixing at the interfaces. Thus, some uncompensated spins at the interfaces are also frozen along the field cooling direction after FC process. With increasing magnetic field, the spiral magnetic order temperature shifts appreciably toward to lower temperature side[16] and the peak involving ferrimagnetic

https://doi.org/10.1557/jmr.2015.272 Published online by Cambridge University Press

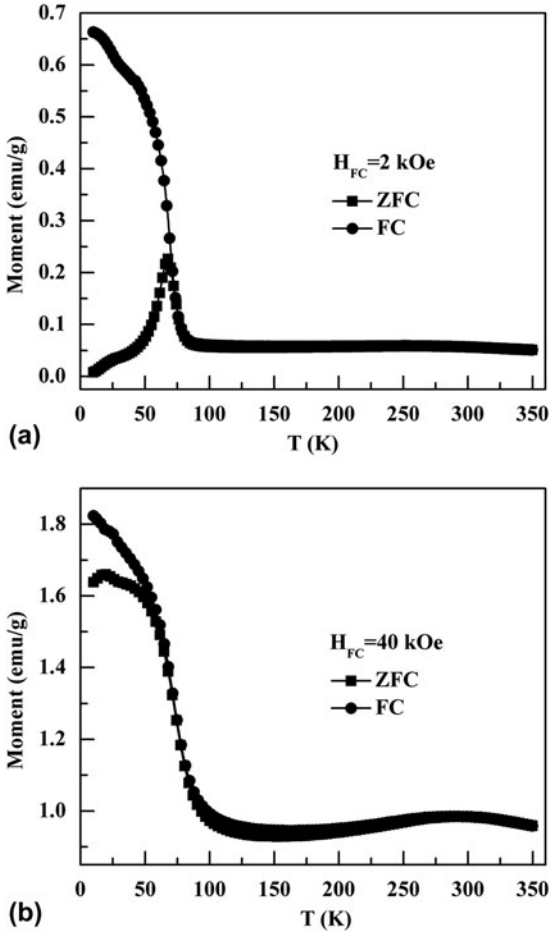


FIG. 2. Temperature dependence of magnetization with ZFC and FC processes at (a) H_{FC} = 2 kOe and (b) H_{FC} = 40 kOe.

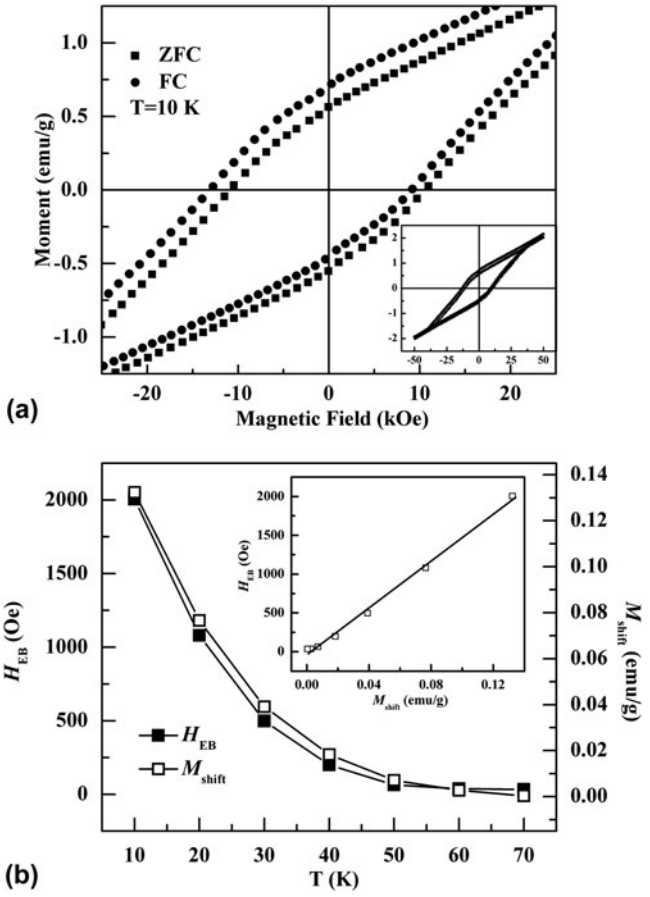


FIG. 3. (a) The ZFC and FC hysteresis loops measured at 10 K cooled from 350 K without applied field and a 30 kOe field, respectively. Inset is the whole loops of ZFC and FC processes. (b) Temperature dependence of H_{EB} and M_{shift} after field cooling in 30 kOe from 350 K and the inset shows the variations in H_{EB} with M_{shift}.

transition is gradually flat, which is probably due to the modification of the interface spins. As discussed above, the interface between $NiCr_2O_4$ and Cr_2O_3 forms into structure disordered layer. The intermediate layer with limited thickness modifies the establishment of long range ordering unlike the original domain in ferrimagnetic and antiferromagnetic phase. The modification results in the asymmetric atomic arrangement and breaks the exchange bonds of magnetic cations. More important, this structural modification can produce competing or pinning interactions between the randomly oriented spins and then the interactions further generate some novel magnetic effects.

Magnetic hysteresis loops have been measured after ZFC and FC processes at 10 K. During ZFC process, the sample was cooled from 350 to 10 K without applied field and for FC process the sample was cooled with a 30 kOe field. After that, hysteresis loops were measured between ±50 kOe. In Fig. 3(a), ZFC magnetic hysteresis loop shows a strict central symmetry at zero field but FC magnetic hysteresis loop exhibits a shift of the loop. Inset of Fig. 3(a) is the whole loops of ZFC and FC processes. We can find that the loops are not saturated evidently even though at high field. However, the system can be considered effectively saturated if the ascending and descending branches of the loop coincide for high fields. We define the field as H_{irr}, above which the loop is closed. In the inset, it shows that the magnetization is reversible in high fields and the loops is closed at H_{irr}, which is about 35 kOe. Ascending and descending branches also have the coincident tendency above the H_{irr}. In other words, the maximum of measuring field is high enough to make hysteresis loop saturate effectively. In addition, ferrimagnetic $NiCr_2O_4$ is commonly easier to get saturation than antiferromagnetic Cr_2O_3. It is reasonable that the $NiCr_2O_4/Cr_2O_3$ system is effectively saturated at higher field than $NiCr_2O_4$. Therefore, those can give the true signature of the observed EB effect, rejecting the minor loop effect. In our system, a negative $H_{EB} \approx 2037$ Oe and a positive $M_{shift} \approx 0.129$ emu/g can be found. Here, H_{EB} is defined as $H_{EB} = (H_{C1} - H_{C2})/2$, where H_{C1} and H_{C2} are the absolute values of left and right coercive fields in the hysteresis loop, respectively.

https://doi.org/10.1557/jmr.2015.272 Published online by Cambridge University Press

M_{shift} is calculated by the mathematical formulae, $M_{shift} = (M_+ - M_-)/2$, in which M_+ and M_- are the absolute values of positive and negative remanent magnetization. Meanwhile, a coercivity enhancement $\Delta H_C \sim 355$ Oe is also observed and H_C is defined as $H_C = (H_{C1} + H_{C2})/2$. Spin disorder at the interface can reduce the antiferromagnetic anisotropy and further influence the coupling strength. With field cooling, interfacial uncompensated spins including frozen and rotatable with different coupling strength can be existed.[17,18] During magnetic reversal, the rotatable antiferromagnetic spins can couple with the adjacent ferrimagnetic moments and follow the ferrimagnetic spin rotation, which can explain the enhancement of H_C. As a pinning center, the frozen antiferromagnetic spins can pin the adjacent ferrimagnetic moment leading to the appearance of H_{EB}. In addition, M_{shift} is another good evidence proving the existence of net uncompensated spins. Some uncompensated spins are pinned along the external field direction and could not rotate following the applied field, which give rises to the appearance of M_{shift} in FC hysteresis loop. Certainly, the value of M_{shift} is depend on the number of pinned spins. Temperature dependence of H_{EB} and M_{shift} is shown in Fig. 3(b). For each measurement, the sample was cooled down from 350 K to the measuring temperature with a 30 kOe field and then the magnetization loops were obtained. As a result, with temperature increasing, H_{EB} and M_{shift} decrease and the values finally tend to zero at 70 K, which is consistent with the irreversible temperature in Fig. 2. Besides, H_{EB} has a similar temperature dependence behavior to M_{shift}. It indicates that they have close correlation and the similar origination. Not only resulting in the generation of M_{shift}, the interfacial frozen uncompensated spins can also act as the pinning layer, execute a microscopic torque on ferrimagnetic spins and then bring about the appearance of H_{EB}. In the inset of Fig. 3(b), nearly linear relationship between M_{shift} and H_{EB} can be noted. It directly reveals the equivalence of the parameters and the value of H_{EB} is determined by the quantity of uncompensated pinned spins on the interfacial layer. The decreasing tendency does not present any anomaly, which can also exclude the influence of spiral magnetic order on EB effect.

In addition, cooling field dependence of H_{EB} and M_{shift} is exhibited in Fig. 4. The sample was cooled down from 350 to 10 K with different field (0.5 kOe $\leq H_{FC} \leq$ 30 kOe). After reaching 10 K, magnetization loops were measured between $\pm$50 kOe. When cooling field increases from 0.5 to 10 kOe, there is an abrupt increase of H_{EB} and M_{shift}. After the initial increase, both of them nearly reach the saturation values. The beginning increase in cooling field just like a stronger applied force induces a growing number of pinned spins along the field

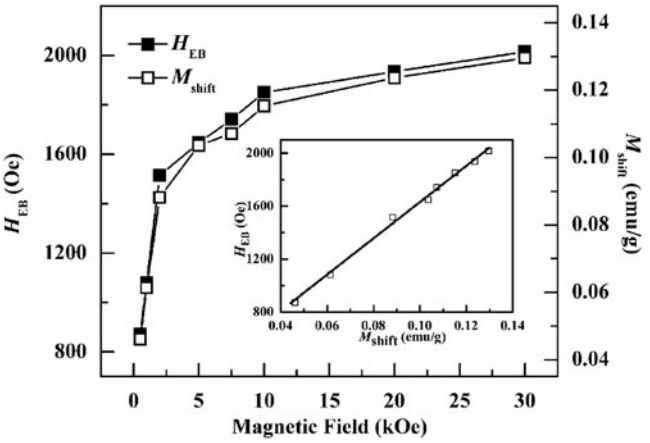


FIG. 4. The cooling field dependence of H_{EB} and M_{shift}, and the inset is the dependence of H_{EB} on M_{shift}.

direction and also induces the increase in M_{shift} and H_{EB}. When cooling field is going on increasing from 10 to 30 kOe, it is high enough to make more pinned spins along the applied field direction and the number of pinned spins varies little with the field. That implies that H_{EB} and M_{shift} obtain the saturated values, and so does the EB effect. From the inset of Fig. 4, the uniform field dependence of H_{EB} and M_{shift} also represents their close relationship and similar origination, which proves the critical role of frozen uncompensated spins in EB effect. Moreover, the EB effect has also been found in single $NiCr_2O_4$ phase.[19,20] Compared with the EB effect of polycrystalline $NiCr_2O_4$ and the nanoparticle phase, the values of H_{EB} and H_C in $NiCr_2O_4/Cr_2O_3$ system are evidently improved. The improvement should be related to the different mechanisms inducing the appearance of EB effect.

One of the interesting characteristics of EB is training effect, which is manifested as the evolution of magnetic hysteresis loop when the system is field-cycled several times successively at a specific temperature. Typically, a gradual decrease of H_{EB} and M_{shift} with increasing number (n) of subsequent loop cycling can be observed. For the training effect measurements, the sample was first cooled from 350 to 10 K under H = 30 kOe. Subsequently, the magnetic hysteresis loops were measured and cycled 9 times, consecutively. As plotted in Fig. 5, training effect is evident in $NiCr_2O_4/Cr_2O_3$ system. The first cycle loop shows a prominent EB effect presenting an asymmetric magnetization reversal characteristic. After that, the subsequent magnetization cycles tend to symmetric gradually. The central part of first, second, and ninth loops are shown in Fig. 5. During the training procedure, both H_{EB} and M_{shift} decrease with the field cycling accompanied with a dramatic decrease in H_{C1} and M_+ in comparison with the variation of H_{C2} and M_-. The systematic decrease of H_{EB} (including H_{C1} and H_{C2}) and M_{shift} with n is shown in Fig. 6. Figure 6(a) proves the

https://doi.org/10.1557/jmr.2015.272 Published online by Cambridge University Press

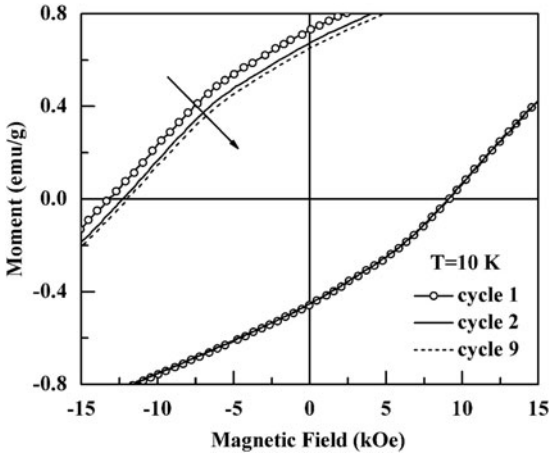


FIG. 5. The first, second and ninth hysteresis loops at 10 K after field cooling from 350 K with 30 kOe.

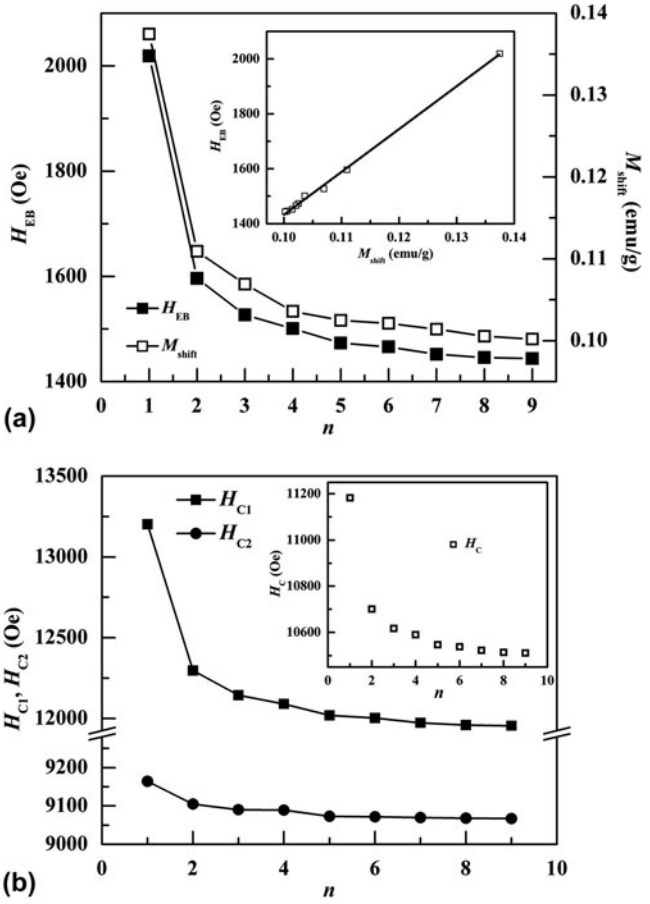


FIG. 6. (a) Field cycle dependence of H_{EB} and M_{shift} at 10 K, and the inset presents the variations of H_{EB} with M_{shift}. (b) Field cycle dependence of H_{C1} and H_{C2} at 10 K, and the inset is the cycle number dependence of H_C.

decrease tendency of H_{EB} and M_{shift}. The inset of Fig. 6 (a) displaying the linear relationship between H_{EB} and M_{shift} is consistent with the inset of Figs. 3(b) and 4. The pinned uncompensated spins at ferrimagnetic/antiferromagnetic interfaces still play a crucial role during training effect. When field cycles are applied continuously, some pinned uncompensated spins try to alter their direction repeatedly along the external field, which results in the depinning at the interfaces between ferrimagnetic and antiferromagnetic phase. Thus, the number of pinned uncompensated spins is gradually decreasing under continuous cycle magnetization and it gives rise to the decrease of M_{shift}. In addition, the decrease tendency of interfacial coupling interaction leads to the decrease in H_{EB}. Therefore, Both H_{EB} and M_{shift} are closely connected with the decreasing fraction of pinned uncompensated spins. As shown in Fig. 6(b), it is not difficult to find that the training effect of H_{EB} is mainly due to the decrease of H_{C1} dependent on n, while H_{C2} just has the uniform tendency with far less evident dependent on n. Furthermore, in spite of the reduction of H_{EB}, H_C also has a shrink with field cycling as plotted in the inset of Fig. 6(b). The different dependence on n of H_{C1} and H_{C2} indicates the different mechanism of magnetization reversal during the left and right branches hysteresis. It is in good agree with the NiO–Fe heterostructure, where coherent rotation is observed at H_{C2} while wall propagation and domain nucleation dominate in the vicinity of H_{C1}.[21]

Figure 7 shows the dependence of H_{EB} on n and the best fitting (solid line) with $n \geq 2$. H_{EB} of the second hysteresis loop (~1600 Oe) is decreased about 20% compared with that of the first loop (~2037 Oe) while the subsequent loops show a more gradual continuous decrease. The distinct character difference of H_{EB} between $n = 1$ and $n \geq 2$ is a signal that training effect in our system is considered to two different explanation. For $n = 1$, magnetization reversal asymmetry may exist, which is correlated with the antiferromagnetic magnetic symmetry due to the onset of biaxial anisotropy. As can be seen in the report by Hoffman,[22] the symmetry of anisotropy in antiferromagnet is crucial for understanding of training effect in EB system. Multiple antiferromagnetic easy anisotropy axes can exist and initially stabilize the noncollinear arrangement of antiferromagnetic spins, which then relaxes into a collinear arrangement after the first magnetization reversal. However, the subsequent field cycles should arise from the conventional mechanism based on the thermally driven depinning of uncompensated spins. The instability of EB system results in a reduction of pinning upon repeated field cycling, which is due to the irreversible changes in the magnetic microstructure of antiferromagnet.[23] To unveil the detailed mechanism, thermal activation and athermal contribution are used to distinct the first and subsequent loops in training effect, recently. The existence of the two types in interfacial domain states after FC has been reported by Chan et al.[24] So, we can explain our training effect through the two types.

https://doi.org/10.1557/jmr.2015.272 Published online by Cambridge University Press

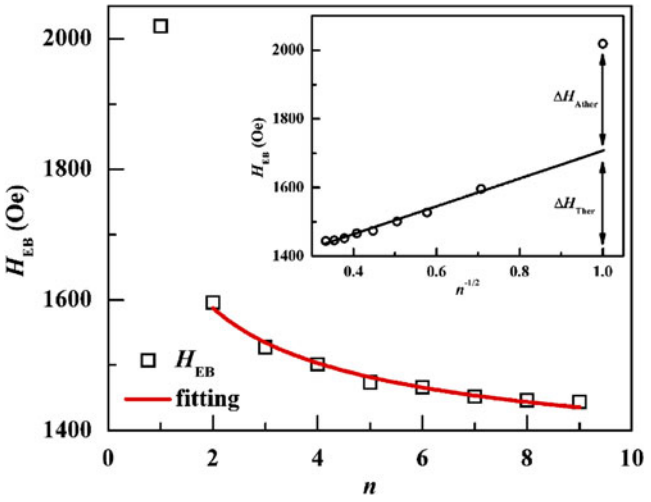


FIG. 7. Field cycle dependence of H_{EB} (open square) and the corresponding best fit (solid line) to the data for $n \geq 2$. The inset is H_{EB} versus $n^{-1/2}$ for $NiCr_2O_4/Cr_2O_3$ system.

For many cases, training effect has been found to obey the empirical $n^{-1/2}$ law. The relationship between H_{EB} and n observed in experimentally is usually expressed by: $H_{EB}^{n} - H_{EB}^{\infty} = \kappa\sqrt{n}$ /, where H_{EB}^{∞} is H_{EB} in the limit of infinite loops and κ is an experimental constant about material dependent decay.[24] As can be seen, the fitting curve in Fig. 7 is in good agree with our experimental data with $n \geq 2$ but fails with $n = 1$. The fitting parameters are $H_{EB}^{\infty} = 1299$ Oe and $\kappa = 406$. According to the thermal activation theory,[25] thermal fluctuations can reduce the stability of antiferromagnetic anisotropy energy and the interfacial exchange energy. As a driving force, ferrimagnetic magnetization reversal can overcome high interfacial pinning energy. Consequently, the reversal of ferrimagnetic moment influences the interfacial ferrimagnetic/antiferromagnetic coupling and leads to the loss of interfacial exchange energy during training cycles. The reduction of interfacial coupling energy is reflected by the decrease of H_{EB} due to the depinning of frozen antiferromagnetic spins. Nevertheless, athermal effect can come from the spin-flop-like coupling and the initial spin configuration cannot be restored. Straight line fitting of H_{EB} versus $n^{-1/2}$ in the inset of Fig. 7 further presents a clear illustration to separate the two effects into athermal and thermal training effect shown as "ΔH_{Ather}" and "ΔH_{Ther}," respectively. Antiferromagnetic phase at the interfaces breaks the adjacent ferrimagnetic phase into small size domains which interact with frozen and rotatable uncompensated spins. The first loop is athermal accompanied with the strong magnetization reversal asymmetry. The subsequent loops have a more gradual loop number dependence and we interpret this contribution as a conventional mechanism due to thermally activated depinning.

IV. CONCLUSIONS

In summary, we have investigated the EB and training effect of $NiCr_2O_4/Cr_2O_3$ system synthesized by a chemical co-precipitation method. With field cooling from 350 to 10 K, magnetic hysteresis loop shows the $H_{EB} \sim 2037$ Oe and $M_{shift} \sim 0.129$ emu/g with a coercivity enhancement $\Delta H_C \sim 355$ Oe. The EB effect disappears near 70 K. This result is attributed to the frozen uncompensated spins and the exchange interaction at the $NiCr_2O_4/Cr_2O_3$ interfaces. During training process, H_{EB} drops abruptly between the first and second magnetic cycles followed by a more gradual continuous change in the subsequent cycles. As suggested, two types of training theories should be existed. One is athermal effect in the first cycle and the other is thermal contribution with the subsequent cycles.

ACKNOWLEDGMENTS

This work is supported by the National Natural Science Foundation of China (Grant Nos. 11174092 and 11474111). We would like to thank the staff of Analysis Center of HUST for their assistance in various measurements.

REFERENCES

1. A.E. Berkowitz and K. Takano: Exchange anisotropy—A review. *J. Magn. Magn. Mater.* **200**, 552 (1999).
2. S. Das, M. Patra, S. Majumdar, and S. Giri: Exchange bias effect at the irregular interfaces between Co and CoO nanostructures. *J. Alloys Compd.* **488**, 27 (2009).
3. W.H. Meiklejohn and C.P. Bean: New magnetic anisotropy. *Phys. Rev.* **102**, 1413 (1956).
4. B. Dieny, V.S. Speriosu, S.S.P. Parkin, B.A. Gurney, D.R. Wilhoit, and D. Mauri: Giant magnetoresistance in soft ferromagnetic multilayers. *Phys. Rev. B* **43**, 1297 (1991).
5. J.C.S. Kools: Exchange-biased spin-valves for magnetic storage. *IEEE Trans. Magn.* **32**, 3165 (1996).
6. R.K. Zheng, G.H. Wen, K.K. Fung, and X.X. Zhang: Training effect of exchange bias in γ-Fe_2O_3 coated Fe nanoparticles. *Phys. Rev. B* **69**, 214431 (2004).
7. S. Guo, W. Liu, H. Meng, X.H. Liu, W.J. Gong, Z. Han, and Z.D. Zhang: Exchange bias and its training effect in Ni/NiO nanocomposites. *J. Alloys Compd.* **497**, 10 (2010).
8. J. Nogués and I.K. Schuller: Exchange bias. *J. Magn. Magn. Mater.* **192**, 203 (1999).
9. V. Skumryev, S. Stoyanov, Y. Zhang, G. Hadjipanayis, D. Givord, and J. Nogués: Beating the superparamagnetic limit with exchange bias. *Nature* **423**, 850 (2003).
10. S.R. Mishra, I. Dubenko, J. Griffis, N. Ali, and K. Marasinghe: Exchange bias effect in ball milled Co–Cr_2O_3 FM–AFM nanocomposites. *J. Alloys Compd.* **485**, 667 (2009).
11. J.B. Yi, J. Ding, Z.L. Zhao, and B.H. Liu: High coercivity and exchange coupling of Ni/NiO nanocomposite film. *J. Appl. Phys.* **97**, 10K306 (2005).
12. M. Ptak, M. Maczka, A. Gagor, A. Pikul, L. Macalik, and J. Hanuza: Temperature-dependent XRD, IR, magnetic, SEM and TEM studies of Jahn–Teller distorted $NiCr_2O_4$ powders. *J. Solid State Chem.* **201**, 270 (2013).

https://doi.org/10.1557/jmr.2015.272 Published online by Cambridge University Press

13. M.R. Suchomel, D.P. Shoemaker, L. Ribaud, M.C. Kemei, and R. Seshadri: Spin-induced symmetry breaking in orbitally ordered $NiCr_2O_4$ and $CuCr_2O_4$. *Phys. Rev. B* **86**, 054406 (2012).
14. T.R. Mcguire, E.J. Scott, and F.H. Grannis: Antiferromagnetism in a Cr_2O_3 crystal. *Phys. Rev.* **102**, 1000 (1956).
15. Z.M. Tian, S.L. Yuan, S.Y. Yin, L. Liu, J.H. He, H.N. Duan, P. Li, and C.H. Wang: Exchange bias effect in a granular system of $NiFe_2O_4$ nanoparticles embedded in an antiferromagnetic NiO matrix. *Appl. Phys. Lett.* **93**, 222505 (2008).
16. M. Tadic, S.M. Savic, Z. Jaglicic, K. Vojisavljevic, A. Radojkovic, S. Prsic, and D. Nikolic: Magnetic properties of $NiMn_2O_{4-\delta}$ (nickel manganite): Multiple magnetic phase transitions and exchange bias effect. *J. Alloys Compd.* **588**, 465 (2014).
17. M. Gruyters and D. Schmitz: Microscopic nature of ferro- and antiferromagnetic interface coupling of uncompensated magnetic moments in exchange bias systems. *Phys. Rev. Lett.* **100**, 077205 (2008).
18. X.P. Qiu, D.Z. Yang, S.M. Zhou, R. Chantrell, K. O'Grady, U. Nowak, J. Du, X.J. Bai, and L. Sun: Rotation of the pinning direction in the exchange bias training effect in polycrystalline NiFe/FeMn bilayers. *Phys. Rev. Lett.* **101**, 147207 (2008).
19. J. Barman, T. Bora, and S. Ravi: Study of exchange bias and training effect in $NiCr_2O_4$. *J. Magn. Magn. Mater.* **385**, 93 (2015).
20. H. Singh, T. Chakraborty, K. Srikanth, R. Chandra, C. Mitra, and U. Kumar: Study of exchange bias in $NiCr_2O_4$ nanoparticles. *Phys. B* **448**, 77 (2014).
21. A. Hochstrat, Ch. Binek, and W. Kleemann: Training of the exchange-bias effect in NiO–Fe heterostructures. *Phys. Rev. B* **66**, 092409 (2002).
22. A. Hoffmann: Symmetry driven irreversibilities at ferromagnetic–antiferromagnetic interfaces. *Phys. Rev. Lett.* **93**, 097203 (2004).
23. D. Paccard, C. Schlenker, O. Massenet, R. Montmory, and A. Yelon: A new property of ferromagnetic–antiferromagnetic coupling. *Phys. Status Solidi* **16**, 301 (1966).
24. M.K. Chan, J.S. Parker, P.A. Crowell, and C. Leighton: Identification and separation of two distinct contributions to the training effect in polycrystalline Co/FeMn bilayers. *Phys. Rev. B* **77**, 014420 (2008).
25. T. Dias, E. Menéndez, H. Liu, C.V. Haesendonck, A. Vantomme, K. Temst, J.E. Schmidt, R. Giulian, and J. Geshev: Rotatable anisotropy driven training effects in exchange biased Co/CoO films. *J. Appl. Phys.* **115**, 243903 (2014).

https://doi.org/10.1557/jmr.2015.272 Published online by Cambridge University Press